

1 Structure-rheology relationship of fully bio-based linear polyester polyols for
2 polyurethanes - synthesis and investigation

3 Paulina Parcheta¹, Janusz Datta^{1,*}

4 ¹ Gdańsk University of Technology, Faculty of Chemistry, Department of Polymers
5 Technology, G. Narutowicza St. 11/12, 80-233 Gdańsk, Poland

6 * Corresponding author (J. Datta): janusz.datta@pg.gda.pl

7 ABSTRACT: The synthesis of polyols from renewable substances as an alternative for
8 petrochemical-based polyols play important matter in the polyurethane industry. In this
9 work, the fully bio-based linear polyester polyols with different catalyst amounts were
10 synthesized via two-step polycondensation method. The effect of various catalyst
11 content on the structure and rheological behavior were established. Fourier Transform
12 Infrared Spectroscopy, Nuclear Magnetic Resonance, Gel Permeation
13 Chromatography and Matrix-Assisted Laser Desorption/Ionization Time-of-Flight mass
14 spectrometry allowed confirming the impact of the catalyst amount during synthesis on
15 the molecular structure of the resulted polyols. Through the hyphenation of these
16 sophisticated polymer characterization techniques, information on the molecular
17 weight distribution was obtained. Moreover, it was found that the obtained polyols are
18 non-Newtonian fluids. According to conducted measurements, it was observed that the
19 poly(propylene succinate)s prepared with the use of the 0.25 wt.% and 0.30 wt.%
20 catalyst revealed the structures and selected properties the most akin to design.

21 KEYWORDS

22 Bio-based poly(propylene succinate); Macromolecular structure; Rheological behavior;
23 MALDI-ToF mass spectrometry; Gel permeation chromatography.

24 1. Introduction

25 Currently, clearly visible is the growing interest of using biorenewables as a
26 primary component at the polymer synthesis. This trend is determined by the
27 unfavorable oil consumption forecasts when the increasing demand for the polymer
28 materials utilization performs on the global market. Recently, the bio-components have
29 become readily accessible which allow producing biopolymers, including polyester
30 polyols even in 100% from bio-resources [1,2]. The biotechnological process
31 consisting of the corn crops fermentation allow obtaining bio-based glycols and
32 dicarboxylic acids. Such microorganisms as fungi, yeasts or bacteria [3–6] lead to the
33 formation of the proper product during fermentation processes.

34 The major advantages which contribute to the increasing interest in the
35 utilization of biorenewables in chemical syntheses [7] represent the reduction of energy
36 consumption, the decrease of the greenhouse gasses production and CO₂ emission
37 reduction. Moreover, the economic volatility reduction by the decrease in the fossil fuel
38 stocks utilization and the decline in the production costs with increasing production
39 scale made a contribution to develop the research on the biorenewables utilization.

40 The initial reaction, which leads to the polyester polyols obtainment, is a two-
41 step polycondensation reaction. The first step constitutes the esterification or
42 transesterification reaction between carboxylic acid or carboxylic acid esters,
43 respectively, and the excess of the glycols. During the esterification, water or alcohols
44 are formed, respectively, as by-products which hindered the main reaction. The
45 capability of the by-product elimination from reaction mixture affected the reaction

46 kinetics and productivity. After the by-product elimination, second step –
47 polycondensation reaction, can be started [8].

48 It is characteristic for this type of polycondensation to run at high temperatures,
49 sometimes exceeding 200°C. However, the choice of temperature depends on the
50 thermal stability of both substrates and the main product. The disadvantages of these
51 methods are often the side reactions to which the oxidation reaction takes place. To
52 prevent these reactions, polycondensation is carried out under inert gas (eg, nitrogen,
53 argon) or under reduced pressure. In addition, the use of both reaction conditions
54 facilitates the removal of the by-product from the reaction medium, thereby shifting the
55 reaction to the main product. It is well-known that the reaction kinetics are also affected
56 by the amount of the catalyst, the chemical structure of the catalyst and monomers,
57 monomer concentration, by the temperature during both steps, reaction time, and
58 removal rate of the low molecular by-products [9]. By manipulating these parameters,
59 we can optimize the polycondensation process to accelerate the formation of the main
60 product [10].

61 Among the industrial properties such as hydroxyl and acidic number and
62 viscosity, the macromolecular structure has also a huge impact on the polyurethane
63 synthesis and properties of resulted materials. Thereby, it is necessary to explore the
64 macromolecular structure of the polyols before polyurethane material synthesis.
65 Recently, the huge interest gained molecular weight distribution study with the use of
66 Matrix-Assisted Laser Desorption/Ionization Time-of-Flight mass spectrometry [11–
67 15]. This method allows obtaining information about absolute molecular weights,
68 identification of mass-resolved polymer chains including intact oligomers, and
69 simultaneous determination of end groups in a polymer sample. Many scientists have
70 used this method to determine the molecular structure of the various type of polymers.

71 Król and Pilch-Pitera [16,17] used this method for structure investigation of urethane
72 oligomers for polyurethane elastomers. The researchers used this method to proposed
73 the majority of molecular structure presented in the materials. They affirmed that not
74 all of obtained bands could be identified in this method but the GPC findings could be
75 confirmed.

76 One of the most important properties which verify polyols possibility to industrial
77 processes is their rheological behavior. Furthermore, rheology can inform about the
78 dynamic viscosity of the fluids, which is important properties during preparation at the
79 used temperature and pressure. The rheological behavior and viscosity are also
80 connected with the structure of the polymer chains [18]. Proposed rheological models,
81 as an optimal individual function, described the fluids rheological behavior. There is
82 two primary behavior delineated the liquids, namely, Newtonian and non-Newtonian.
83 The Newtonian model characterizes the ideal fluids, which performed linear curve
84 course in the rheograms, which show the shear stress via shear rate (dynamic viscosity
85 stay constant for all point of the curve). This model is described by the equation (1):

$$86 \quad \tau = \eta * \gamma \quad (1)$$

87 Where: τ – shear stress [Pa], γ – shear rate [s^{-1}], η – viscosity [Pas].

88 Non-Newtonian fluids are described by a large number of models. This type of
89 fluids does not show the linearity of the curve course in the rheograms. The non-
90 Newtonian liquids exhibit the complex structure, and due to the various deformation
91 effects, they can be characterized as pseudoplastic fluids, viscoplastic, dilatant or
92 thixotropic liquids. There are several mathematical models which allow describing the
93 information about the non-Newtonian fluids rheological behavior. There are three

94 mostly applied models: Herschel, Bulkley, Ostwald-de Waele and Bingham models
95 [19]. For the test analysis, two of them will be characterized.

96 The Herschel, Bulkley model, describe the fluids with a nonlinear rheograms.
97 The model is expressed by the equation (2):

$$98 \quad \tau = \tau_0 + K * \dot{\gamma}^n \quad (2)$$

99 Where: τ – shear stress [Pa], τ_0 – yield stress [Pa], $\dot{\gamma}$ – shear rate [s^{-1}], K – consistency
100 index [-], which gives an idea of the fluid viscosity, n – flow behavior index [-], which
101 should be similar to comparative study of the different fluids. The ' τ_0 ' and ' n ' values
102 give information about fluids behavior as follows:

103 $\tau_0 = 0, n = 1$ – means that the Herschel, Bulkley mathematical model describes the
104 Newtonian behavior of the fluids;

105 $\tau_0 = 0, n > 1$ – the Herschel, Bulkley mathematical model describes the dilatant
106 behavior (shear thickening);

107 $\tau_0 = 0, n < 1$ – the Herschel, Bulkley mathematical model describes the behavior of the
108 pseudoplastic fluid (shear thinning);

109 $\tau_0 > 0, n = 1$ – the Herschel, Bulkley mathematical model describes the Bingham
110 plastics, which are the fluids with the linear viscosity curve above the yield stress [19].

111 The Ostwald-de Waele describe the shear thinning fluids without a yield stress.

112 The model is expressed by the equation (3):

$$113 \quad \tau = K * \dot{\gamma}^{(n-1)} \quad (3)$$

114 Where: τ – shear stress [Pa], $\dot{\gamma}$ – shear rate [s^{-1}], K – consistency index [-] gives an
115 idea of the fluid viscosity, n – flow behavior index [-] which give information about fluids
116 behavior as follows:

117 $n < 1$ – pseudoplastic,

118 $n = 1$ – Newtonian fluids,

119 $n > 1$ – dilatant fluids [19].

120 Schrock and co-workers [20] investigated the structure, thermal phase transition
121 temperatures and viscosity of few polyester polyols prepared based on succinic acid,
122 adipic acid and various glycols. Materials were synthesized with planned average
123 molecular structure at ca. 1000 and 2000 Da. They explored that the poly(propylene
124 succinate)s polyesters and co-polyester with other glycols revealed high viscosity even
125 at elevated temperature. Schrock investigated that the viscosity value of pure
126 poly(propylene succinate) at 80°C revealed ca. 1000 mPas. Our work presents the
127 impact of the catalyst employment during synthesis on the viscosity of poly(propylene
128 succinate) and other properties.

129 In this work, the synthesis of fully bio-based poly(propylene succinate)s via well-
130 known two-step polycondensation method is described. The polycondensation
131 catalyst, tetraisopropyl orthotitanate TPT, was used to find the catalyst impact on the
132 structure and rheological behavior. Six poly(propylene succinate)s were analyzed by
133 Fourier Transform Infrared Spectroscopy and Nuclear Magnetic Resonance. The
134 structure was also verified by Gel Permeation Chromatography, which characterizes
135 the impact of the catalyst amount on the molecular weight distribution. Moreover, for
136 more detailed investigation, the study of the molecular weight distribution was



137 expanded about results of the Matrix-Assisted Laser Desorption/Ionization Time-of-
138 Flight mass spectrometry. The influence of the catalyst amount on the rheological
139 behavior was determined with the use of rotary rheometer. The choice of the
140 measurements temperature ranges and shear rates were done due to the temperature
141 conditions for industrial processes during preparation and production of polyurethane
142 materials [18].

143 2. Materials and methods

144 2.1. Materials

145 The main components used in this study:

146 Bio-based succinic acid (SA) was obtained from BioAmber Sarnia Inc. (Ontario,
147 Canada) as a solid-state component with purity in the range 98-100%. The molecular
148 weight was 118.09 g/mol and relative density at 20°C was 0.900 g/cm³.

149 Susterra Propanediol (1,3-propanediol) was obtained from DuPont Tate&Lyle
150 Corporation Bio Products (Loudon, Tennessee, USA) as a liquid component with purity
151 ca. 99.98%. The molecular weight was 76.09 g/mol, and relative density at 20°C was
152 1.053 g/cm³. Moreover, water content by Karl Fischer equaled 12.1 ppm and a dynamic
153 viscosity at 20°C was 52 mPas.

154 Tetraisopropyl orthotitanate, Ti(O-i-Pr)₄ (TPT) was purchased from TCI Chemicals
155 (India) as a liquid with the purity ca. 97% and the molecular weight: 284.22 g/mol and
156 was used as a catalyst with four different amount.

157 For the analytical measurement methods, other materials and solvents were used
158 of analytical grade.



159 2.2. Bio-based polyesters synthesis

160 Aliphatic bio-based polyester polyols – poly(propylene succinate)s, were prepared
161 with the use of succinic acid SA and 1,3-propanediol PDO, both with a natural origin.
162 Catalyst, tetraisopropyl orthotitanate TPT, was used as a glycol equivalent in five
163 different amount, namely, 0.1 wt.% (PPS-0.10), 0.15 wt.% (PPS-0.15), 0.2 wt.% (PPS-
164 0.20), 0.25 wt.% (PPS-0.25) and 0.30 wt.% (PPS-0.30). The reference sample was
165 prepared without catalyst employment (PPS-0.00). All aliphatic bio-based polyester
166 polyols were synthesized by two-step polycondensation method, which scheme is
167 shown in Figure 1. The first step was represented by the esterification reaction between
168 a succinic acid (SA) and 1,3-propanediol (PDO). Glycol was always used with an
169 excess and the molar ratio SA: PDO amounted to 1:1.2. Determination of this molar
170 ratio was ordered by the final molecular weight expected after full polycondensation.
171 The expected number average molecular weight of the prepared bio-based polyester
172 polyols was $M_n = 2000$ g/mol with functionality equaled 2, for proving linearity in the
173 molecular structure. The reaction was carried out in the glass reactor, which consisted
174 of a three-neck flask equipped with nitrogen/vacuum inlet, mechanical stirrer,
175 thermometer, condenser, and heating mantle. The first step of the reaction was carried
176 out under a nitrogen atmosphere. The bio-based component mixture was stirring at
177 140°C and after water distillation, the second step was started according to the patent
178 application in the Polish Patent Office (no. P.418808). During the polycondensation
179 reaction, the nitrogen was stopped, the appropriate amount of catalyst was added, and
180 the temperature was increased up to 160°C under reduced pressure. The acidic
181 number was measured to track the reaction progress. After achieving the value of the
182 acidic number ca. or preferably below 1 mg KOH/g, the polycondensation was finished.

183

184 Figure 1 Two-step polycondensation method for poly(propylene succinate)
185 obtainment.

186

187 2.3. Polymer characterization

188 2.3.1. Acidic and hydroxyl number

189 Carboxyl end-group value measurements were performed by the Polish
190 standard PN-86/C45051. Samples about 1 g of the prepared polyesters were dissolved
191 in ca. 30 cm³ of acetone at room temperature. After that, the solutions were titrated
192 with the use of a standard solution of potassium hydroxide KOH in distilled water (0.1
193 mol/dm³) and phenolphthalein as indicator.

194 Hydroxyl end-group determination was prepared by the Polish standard PN-
195 88/C-89082. Sample about ca. 0.5 g of polyester was dissolved in 5 cm³ of the acetic
196 anhydride solution. The solution was refluxed for 30 minutes. Subsequently, 1 cm³ of
197 pyridine was added and heating for 10 minutes. After that, 50 cm³ of distilled water was
198 added, the mixture was cool to room temperature and titrated with the use of a standard
199 solution of potassium hydroxide KOH in distilled water (0.5 mol/dm³) and
200 phenolphthalein as indicator.

201 2.3.2. Dynamic viscosity

202 Dynamic viscosity measurements were performed with the use of rotary
203 rheometer R/S-CPS+ produced by Brookfield Company, USA. The viscosity values at
204 70 and 80°C were defined with the use of computer program Rheo3000.
205 Measurements were conducted with controlled shear rate (CSR). Justification of
206 choice the temperature is occurring temperature ranges in some industrial processes.



207 2.3.3. Fourier Transform Infrared Spectroscopy (FTIR)

208 Fourier Transform Infrared Spectroscopy was used to obtain the spectra of the
209 bio-based polyester polyols and pure components (1,3-propanediol and succinic acid).
210 The measurements were carried out using a Nicolet 8700 FTIR spectrometer (Thermo
211 Electron Corporation, USA) with the use of ATR technique. Sixty-four scans in the
212 wavenumber range from 4500 to 500 cm^{-1} were taken with the resolution 4 cm^{-1} .

213 2.3.4. Nuclear magnetic resonance (^1H NMR)

214 Proton nuclear magnetic resonance (^1H NMR) spectra of the prepared bio-
215 based polyester polyols were obtained with the use of Bruker spectrometer. Operating
216 frequency was 400 MHz for protons. The ca. 10% w/v solutions of the poly(propylene
217 succinate) polyesters were prepared in a CDCl_3 solvent at ambient temperature. The
218 simulation and iteration of spectra were carried out using Bruker software.

219 2.3.5. Gel permeation chromatography (GPC)

220 Molecular weight distribution of the synthesized bio-based polyester polyols was
221 determined with the use of Gel permeation chromatography, GPC. Measurements
222 were performed using a Thermo Scientific chromatograph, equipped with an isocratic
223 Dionex UltiMate 3000 pump and a RefractoMax 521 refractive index detector. Four
224 Phenogel GPC columns, produced by Phenomenex, were used with 5 μm particle size
225 and 10^5 , 10^3 , 100 and 50 \AA porosities, respectively, located in an UltiMate 3000
226 thermostatic column compartment. The separation was carried out at 30°C.
227 Tetrahydrofuran (THF) was used as mobile phase at a flow rate of 1 mL/min. Bio-
228 Based polyester polyol specimens were prepared by dissolving in THF at 1 wt.% and
229 filtering using nylon filters with 2 μm pore size. Number-average molecular weight, M_n ,



230 weight-average molecular weight, M_w and polydispersity, PD were determined as
231 polystyrene standards.

232 2.3.6. Matrix-assisted laser desorption/ionization time-of-flight mass spectrometry 233 (MALDI-TOF MS)

234 Matrix-assisted laser desorption/ionization time-of-flight mass spectrometry
235 (MALDI-TOF MS) was used to determine the comprehensive structure analysis all of
236 the prepared bio-based polyester polyols. The MALDI-TOF MS spectra were recorded
237 on an AXIMA Assurance Linear MALDI-TOF Mass Spectrometer (Shimadzu Scientific
238 Instruments (SSI), Kyoto, Japan) equipped with near-axis N_2 laser irradiation with
239 variable repetition rate 50 Hz in positive linear mode. Typically, 100 single-shot
240 acquisitions were summed to give a sample mass spectrum. All data were reprocessed
241 using the PolymerAnalysis™ software. The matrix, 2,5-dihydroxybenzoic acid (DHB),
242 was dissolved in tetrahydrofuran (THF) (ca. 10 mg/mL). As cationizing agent was used
243 a potassium salt of fluoroacetic acid (CH_2FCOOK) in THF. The solution of matrix,
244 cationizing agent and the polymer solution (5 mg/mL in tetrahydrofuran) was mixed in
245 a 1:10:5 v/v ratio. Approximately 1 μ L of the final mixture was spotted onto a stainless
246 steel MALDI plate and allowed to dry before insertion into the ion source. Mass
247 spectrometry analysis proved to be a highly effective tool to facilitate the identification
248 of the molecular structure distribution of the prepared bio-based polyester polyols as
249 well as serve as a core method to investigate the impact of the catalyst amount on the
250 polyols structure development during synthesis.

251 2.3.7. Rheological behavior

252 Rheological measurements were performed with the use of rotary rheometer
253 R/S-CPS+ produced by Brookfield Company, USA. The machine was equipped with



254 the cone/plate system. The rheological models and parameters were defined and
255 calculated with the use of computer program Rheo3000. Measurements were
256 conducted with controlled shear rate (CSR). All samples were tested by the program
257 where first the increasing shear rate was conducted from 0 to 100 s⁻¹ for 120 s, in the
258 next step the constant shear rate for 120 s was applied and at the end, the decreasing
259 shear rate from 100 to 0 s⁻¹ for 120 s were carried out. Based on the rheological
260 measurements, the viscosity and flow curves of synthesized bio-based polyester
261 polyols and commercially used polyester polyol POLIOS 55/20 (Purinova Sp. Z o.o.,
262 Bydgoszcz, Poland) were plotted at temperatures 60, 70 and 80°C. Justification of the
263 conditions choice is occurring shear rate ranges and processing temperatures in some
264 industrial processes [18,21]. Moreover, it gave the possibility to more comprehensive
265 comparative study between particular samples.

266 3. Results and Discussion

267 3.1. Synthesis and characterization of the obtained poly(propylene succinate)s

268 All prepared polyester polyols were synthesized with the use of well-known two-
269 step polycondensation method. The first step was the esterification reaction, which was
270 conducted for 10 hours for all of the prepared polyester polyols without catalyst used.
271 After minimum 60% of water removal, the catalyst was added. The second step, which
272 was the main polycondensation reaction, was carried out by individual time for all
273 synthesized polyesters until achievement the acid number ca. or preferably lower than
274 1 mg KOH/g. Justification of choice the end-point of the polycondensation reaction was
275 the carboxyl end group value due to the acid number occurring in some synthetic
276 polyester polyols commonly used in the polyurethane industry [22]. Table 1 shows the
277 preparation condition and properties of the obtained bio-based polyester polyols.



278 Table 1 Preparation and properties of the obtained bio-based polyester polyols and
 279 POLIOS 55/20.

POLYOL	PPS- 0.00	PPS- 0.10	PPS- 0.15	PPS- 0.20	PPS- 0.25	PPS- 0.30	POLIOS 55/20
MOLAR RATIO SA: PDO			1:1.2				ND
CATALYST CONTENT [wt.%]	0.00	0.10	0.15	0.20	0.25	0.30	ND
ESTERIFICATION REACTION TIME [h]			10				ND
POLYCONDENSATION REACTION TIME [h]	170	35	15	10	9	10	ND
ACID NUMBER [mg KOH/g]	1.16	0.97	0.84	0.92	0.83	0.91	0.30
HYDROXYL NUMBER [mg KOH/g]	44.6	64.2	50.4	61.8	51.5	74.9	58.0
VISCOSITY [80°C, Pas]	100*	4.35	6.17	8.87	3.43	2.88	2.20

280 ND – not defined; * Dynamic viscosity measured at 90°C

281 The final properties of the synthesized polyester polyols showed the significant
 282 impact of the catalyst usage. With the growing catalyst amount, the polycondensation
 283 reaction time was decreased up to 0.25 wt.% catalyst usage. The lack of the second
 284 step time reduction was visible for the sample with the highest catalyst content (PPS-
 285 0.30). Nevertheless, sample PPS-0.30 characterized viscosity value more akin to
 286 commercially used polyester polyols POLIOS 55/20.

287 The value of the hydroxyl number confirmed similarity of the prepared bio-based
 288 polyester polyols to the commercially used synthetic polyester polyols proposed for
 289 flexible and thermoplastic polyurethane materials (e.g.: POLIOS 55/20, PURINOVA
 290 Sp. Zoo, Bydgoszcz, Poland) [22].

291 The viscosity of the synthesized polyester polyols also verified the influence of
 292 the catalyst employment on the polyol final properties. Without catalyst usage, the
 293 synthesized polyester polyol revealed the highest viscosity, 100 Pas at 90°C (Table 1).

294 This viscosity level disallows PPS-0.00 usage in the industrial processes. With the
295 growing catalyst usage during poly(propylene succinate)s synthesis, the increasing
296 tendency at the viscosity until 0.20 wt.% catalyst content was observed. For polyols
297 prepared with the use of 0.25 and 0.30 wt.% catalyst content, the viscosity was
298 decreased. The lowest value revealed sample containing the highest catalyst content
299 (PPS-0.30: 2.88 Pas at 80°C), but the polycondensation reaction time was longer than
300 the PPS-0.25 polyol.

301 3.2. Structure analysis

302 The structure analysis was performed using the FTIR and ^1H NMR
303 measurements. The Fourier Transform Infrared spectra of the poly(propylene
304 succinate)s and pure component used for polyesters synthesis (1,3-propanediol and
305 succinic acid) are shown in Figure 2. The broad peak characteristic for the 1,3-
306 propanediol spectrum in the wavelength range between 3570 and 3170 cm^{-1} was
307 attributable to the stretching vibrations of hydrogen-bonded hydroxyl groups. For the
308 succinic acid spectrum, the peak assigned to the hydrogen-bonded carboxyl groups
309 stretching vibration appeared as the broad peak centered at 3300-2500 cm^{-1} . The
310 peaks at 3000-2850 cm^{-1} were assigned to the methylene groups which are visible for
311 glycol and polyesters spectra. Two intensive peaks visible for poly(propylene
312 succinate) spectrum at 1725 cm^{-1} and 1150 cm^{-1} indicated ester groups [23]. The peak
313 at 1725 cm^{-1} is assigned to carbonyl group stretching vibration related to the ester
314 groups from synthesized polyester polyols. The peak at 1690 cm^{-1} visible on the
315 succinic acid spectrum also indicated the $-\text{C}=\text{O}$ stretching vibration but assigned to
316 the carboxyl group. The absorption at 1150 cm^{-1} is related to the $\text{C}(\text{O})-\text{O}-\text{C}$ stretching
317 vibration from the formed ester groups. The two clearly visible peaks at 1380 and 1400



318 cm^{-1} ascribed the -OH bending vibration derived from succinic acid. The peaks at 1170
319 cm^{-1} on the glycol spectrum and 1200 cm^{-1} on the succinic acid spectrum are attributed
320 to the -C-O group stretching vibration [24]. The bond in the wavenumber at 1030 cm^{-1}
321 indicated -C-O stretching vibration from synthesized polyesters and 1.3-propanediol
322 [25].

323 In the case of analyzed poly(propylene succinate)s, the intensity of the peaks,
324 which are assigned to the ester groups (wavenumber: 1725 cm^{-1} and 1150 cm^{-1}), is
325 similar. The results allowed confirming that the content of the catalyst nonsignificantly
326 influenced on the macromolecular structure of the synthesized polyols.

327

328 Figure 2 FTIR spectra of the used succinic acid, 1.3-propanediol, and selected
329 poly(propylene succinate)s.

330

331 ^1H NMR spectra were used to study the structure of the synthesized polyesters
332 (Figure 3). Based on the spectra of the poly(propylene succinate)s prepared with the
333 0.15, 0.20 and 0.25 wt.% catalyst employment, the chemical shifts of the protons were
334 investigated. The characteristic intensive single peak at 2.63 ppm is attributed to
335 methylene protons 'd' from succinic acid (-CH₂-C(O)-) [26,27]. Peaks marked 'e' (-CH₂-
336 O-) and 'f' (-CH₂-) at 4.20 and 2.00 ppm, respectively, are connected with a triple and
337 multiple peaks corresponding to methylene protons from propylene glycol (1.3-
338 propanediol) [28,29]. At the sample spectra are also visible other peaks in lower
339 intensity which can indicate the end groups of oligomers. The little triple peak at 3.65
340 ppm named 'a' attributed to methylene protons from hydroxyl-terminated ends (-CH₂-



341 OH) of polyester macromolecules [30]. The peak at 4.35 ppm named 'c' is attributed
342 to the triple peak corresponding to methylene protons (-CH₂-O-) from glycol terminated
343 ends group. Peak named 'b' at ca. 1.90 ppm is connected to methylene protons also
344 from glycol terminated ends group (-CH₂-). Chrissafis and co-workers [28] explain that
345 these little shifts at the 1.90, 3.68 and 4.35 ppm can correspond to the low molecular
346 weight of the synthesized polyester polyols. These peaks verified the intensity of the
347 polyester macromolecules end-groups occurrence. At the ¹H NMR spectra of the high
348 molecular weight polyesters, these shifts are not visible.

349

350 Figure 3 ¹H NMR spectrum of the synthesized poly(propylene succinate)s samples.

351

352 3.3. Gel permeation chromatography measurements

353 Molecular weight distribution depended on the reaction condition such as used
354 temperature, pressure, stirring but also on the molar ratio of the components and the
355 used catalyst. The gel permeation chromatography was measured to characterize the
356 number average molecular weight and polydispersity of the synthesized polyester
357 polyols. The impact of the catalyst amount on the molecular structure is shown in
358 Figure 4. Table 2 presents the statement of the GPC results. For better results
359 exposition the POLIOS 55/20 was used as a reference sample [31]. It is commercially
360 used synthetic polyester polyol proposed for the flexible and thermoplastic
361 polyurethane materials (PURINOVA Sp. Zoo, Bydgoszcz, Poland). POLIOS 55/20
362 reveals number average molecular weight at ca. 2000 g/mol. The distinct peaks at
363 similar retention time for all measured polyols are visible on the graph. It is seen that
364 with the catalyst amount during the polycondensation reaction the synthesized polyols

365 revealed more akin to designed average molecular weight and lower polydispersity.
366 With the growing catalyst content, the prepared materials exhibit the retention time
367 similar to the reference sample – POLIOS 55/20 and thereby more coterminous
368 average molecular weight.

369 Polyol named PPS-0.00, which was prepared without catalyst employment
370 exhibited the sharp peak at the shortest retention time. It verified the highest average
371 molecular weight of prepared bio-based polyester polyols. Although the single peak at
372 the graph (Figure 4), PPS-0.00 revealed the highest polydispersity which indicates the
373 high dispersion of molecular weight on the polyol structure. The polydispersity of PPS-
374 0.00 amounts to 3.5235. The usual level of the molecular weight dispersion should be
375 equaled ca. 1.05-2.0. It can be account for the lower molecular weight macromolecules
376 distribution in the sample. The smaller macromolecules reveal higher retention time
377 and thereby they are unseen at the used retention time range on the graph.

378 In the case of the PPS-0.10 polyol where the 0.10 wt.% of TPT was used, the
379 final polyol revealed double-peak at the graph of the average molecular weight
380 distribution. It indicates the long chain macromolecules distribution on the sample and
381 high polydispersity level. The first peak indicates the M_n at ca. 18 000 g/mol, when the
382 second peak – ca. 2500 g/mol. The polydispersity at the second peak equaled 1.9640
383 which is also very high. It confirmed the above-mentioned assumptions involved PPS-
384 0.00 polyol. This catalyst amount is deficient for polyol with good polydispersity and
385 planned average molecular weight preparation.

386 The catalyst addition above 0.10 wt.% allowed the polyester polyol synthesis
387 with the beneficial molecular weight distribution. Polyols PPS-0.15, PPS-0.20, PPS-
388 0.25 and PPS-0.30, revealed coterminous number average molecular weight with the



389 expected (2000 g/mol). Nevertheless, polyols prepared with the 0.15 and 0.20 wt.%
 390 catalyst content exhibited high polydispersity level, above 2.0. Bio-based
 391 poly(propylene succinate) synthesized with the 0.30 wt.% catalyst content revealed the
 392 best molecular weight distribution with the ca. 1.8 polydispersity level and ca. 2000
 393 g/mol number average molecular weight. It can be explained as catalyst content which
 394 shifts the reaction towards a product with planned average molecular weight with the
 395 best efficiency from measured polyols. A detailed study of the structures of the different
 396 polyols detected by GPC was performed by MALDI-TOF MS in order to identify the
 397 eventual side reactions producing differences in the molecular weight distribution.

398

399 Figure 4 GPC spectra of the synthesized poly(propylene succinate)s.

400

401 Table 2 The results of the GPC measurements.

BIO-BASED POLYESTER POLYOL	M _n	M _w	PDI
PPS-0.00	4615	16261	3.524
PPS-0.10	18270/2524	18903/4957	1.035/1.964
PPS-0.15	22705/2050	24527/4752	1.080/2.318
PPS-0.20	1727	4466	2.586
PPS-0.25	2578	4644	1.801
PPS-0.30	2158	3808	1.765
POLIOS 55/20*	2000	3349	1.675

402 *reference sample – commercially used linear synthetic polyester polyol proposed for the flexible and
 403 thermoplastic polyurethane materials, PURINOVA Sp. zoo, Bydgoszcz, Poland

404 3.4. MALDI-ToF mass spectrometry

405 Matrix-assisted laser desorption/ionization time-of-flight (MALDI-ToF) mass
 406 spectrometry is a powerful method for the characterization of polymers [12,16,32].

407 MALDI-ToF MS as a soft ionization method provides measurements of absolute
408 molecular weights, identification of mass-resolved polymer chains including intact
409 oligomers and simultaneous determination of end groups in polymer sample [33]. Four
410 representatives bio-based poly(propylene succinate) samples were measured with the
411 use of MALDI-ToF mass spectrometry. The study of their structure was investigated in
412 terms of the presence and possible domination of a specific oligomer, polymerization
413 degree and end groups. Moreover, MALDI-ToF measurements give information about
414 macromolecular weight distribution. Similar to GPC, there is an ideal situation when
415 MALDI-ToF spectra (peak profiles) have approximate Gaussian curve [17].

416 The MALDI-TOF mass spectra were obtained at the m/z range from 450 to 9000
417 Da, what gave peaks with various polymerization degree from 2-3 even to 40 and more
418 (Figure 5). Presented signals correspond to the K^+ doped macromolecules. The
419 distance between the main peaks amount to 158 Da, which is connected with the
420 molecular weight of the bio-based poly(propylene succinate) repeating units. Obtained
421 spectra include also peaks which are related to oligomers displayed other chemical
422 structure than designed. It is visible that all of the measured polyols revealed
423 differences in the curve courses. Due to the various catalyst amounts during the
424 polycondensation process between succinic acid and the excess of the 1,3-
425 propanediol, the various molecular mass distributions are observed.

426

427 Figure 5 MALDI-ToF spectra of the bio-based poly(propylene succinate)s: a) PPS-
428 0.00, b) PPS-0.10, c) PPS-0.15, d) PPS-0.20, e) PPS-0.25, f) PPS-0.30.

429

430 Sample PPS-0.00 (Figure 5 a) is characterized by peak profile with two broad
431 spectra with maximum intense at 1147 Da, within 39 Da from K^+ ($M+K^+$) which indicate
432 polymerization degree 7 ($n=7$), and 4704 Da ($n=29$, $M+K^+$) in the m/z range from 500
433 to 6000 Da. Furthermore, a lot of peaks are visible in the m/z range from 500 to 2500
434 Da. These peaks are related to different molecular chain structure, specifically, with
435 various end groups of the synthesized oligomers in the polyol PPS-0.00. The spectrum
436 course departs from Gaussian distribution, thus the results of the MALDI-ToF
437 measurements confirmed the macromolecular weight distribution from the GPC,
438 exactly, high polydispersity. Bio-based poly(propylene succinate) prepared with the
439 catalyst usage at 0.10 wt.% revealed more similar spectrum to Gaussian curve (Figure
440 5 b) in the m/z range from 500 to 8500 Da. This sample has a maximum at 1696 Da
441 ($n=10$, $M+K^+$), but the most intensive peak is visible at 615 Da ($n=3$, $M+K^+$) which is
442 connected with molecules terminated by acid-end groups. Samples PPS-0.15 and
443 PPS-0.30 (Figure 5 c and f) revealed similar spectra shape. The first from above-
444 mentioned polyols characterized peaks in the m/z range from 500 to ca. 6500 Da,
445 second polyols - from 500 to ca. 6000 Da. The most intensive peaks in both cases are
446 at 747 and 746 Da ($n=4$, $M+K^+$), respectively. The difference is related to the carbon
447 isotope occurrence at the polyol macromolecules. These peaks confirmed
448 macromolecules formation with hydroxyl-terminated end groups. Sample PPS-0.30
449 has more complicated structure due to peaks occurrence in the m/z range from 500 to
450 1000 Da (Figure 5 f). PPS-0.20 is characterized by the most similar peak profile to
451 Gaussian curve (Figure 5 d). The maximum intense at 2486 Da ($n=15$, $M+K^+$) confirms
452 hydroxyl-terminated macromolecules occurrence. Polyol PPS-0.25 has similar peak
453 profile to PPS-0.20 but with a visible double maximum at 1853 ($n=11$, $M+K^+$) and 5966
454 Da ($n=37$, $M+K^+$). Theoretical bio-based poly(propylene succinate) should have



455 polymerization degree ca. 12 for obtaining designed macromolecular weight. More
 456 precise spectra interpretation of selected polyol samples is presented in Table 3.
 457 Table 3 Interpretation of MALDI-ToF mass spectra for obtained bio-based polyester
 458 polyols.

Bio-based poly(propylene succinate)	Location of band (m/z) (M+K ⁺)	Polymerization degree (n)	Probable structure of molecule (M-K ⁺)	Calculated molecular weight (M+K ⁺) [g/mol]
PPS-0.00	513.97	3	A	513.31
	582.58	3	PPS	587.34
	672.27	4	A	671.38
	830.54	5	A	829.45
	906.94	5	PPS	903.48
	976.48	5	ND	ND
	988.82	6	A	987.52
	1147.03	7	A	1145.59
	1305.11	8	A	1303.66
	1323.02	7	A-SA-PDO	1321.77
	1363.30	8	ND	ND
	1463.10	9	A	1461.73
	1538.96	9	PPS	1535.76
	1621.04	10	A	1619.80
	1638.94	9	A-SA-PDO	1637.91
	1696.91	10	PPS	1693.83
1854.91	11	PPS	1851.90	
Peaks from 2012.95 to 4704.99 Da and further are related to macromolecules PPS with higher polymerization degree (from 12 to 29 and further).				
PPS-0.20	193.48	1	A	197.17
	317.76	1	[A-SA-H ₂ O] ⁻	315.26
	355.77	2	A	355.24
	423.64	2	PPS	429.27
	615.62	3	A-SA	613.40
	807.58	4	ND	ND
	1038.29	6	ND	ND
	1064.35	6	PPS	1061.61
	1222.41	7	PPS	1219.62

Peaks from 1222.41 to 7226.15 Da and further are related to macromolecules PPS with higher polymerization degree (from 7 to 45 and further).

PPS-0.25	354.99	2	A	355.24
	422.88	2	PPS	429.27
	430.92	2	PPS	429.27
	747.09	4	PPS	745.41
	905.22	5	PPS	903.48
	1063.30	6	PPS	1061.61
	1221.32	7	PPS	1219.62
	1303.37	8	A	1303.66
	1379.50	8	PPS	1377.69

Peaks from 1379.50 to 8023.62 Da and further are related to macromolecules PPS with higher polymerization degree (from 8 to 50 and further).

459 *ND – not defined;

460 *A, A-SA, A-SA-PDO, [A-SA-H₂O], PPS– structures of macromolecules (see Figure 6).

461 Table 3 shows the precise interpretation of MALDI-ToF spectra of three selected
 462 poly(propylene succinate)s. All of the peaks at characteristic m/z ranges represent
 463 macromolecules with a specific structure and specific end-groups. From obtained data,
 464 it was possible to calculate the polymerization degree (n) and molecular weight of the
 465 probable structure of a molecule for several peak locations. All defined structures are
 466 coded and presented in Figure 6. At all of the prepared bio-based poly(propylene
 467 succinate)s it was desirable to obtain the highest amount of the PPS structures
 468 throughout the sample volume. These macromolecules are hydroxyl-terminated from
 469 both sides. Structure A is related to macromolecules terminated by both, an acid-end
 470 group as well as an hydroxyl-end group. A-SA-PDO describe features when hydroxyl-
 471 terminated macromolecules are formed but during ionization differently detected
 472 macromolecules are formed. Structure A-SA depicts macromolecules terminated by
 473 acid-end groups from both sides. MALDI-ToF measurements can lead to complex
 474 structure formation, even with residual water which can be presented in the sample.
 475 This possible situation described probable structure coded A-SA-H₂O. It is

476 characteristic that the most ordered structure (the most approximate to designed)
477 revealed sample PPS-0.25. The results of the MALDI-ToF mass spectrometry
478 confirmed the results obtained from GPC measurements. Sample PPS-0.25 revealed
479 the lowest polydispersity and the most ordered and approximate to designed,
480 macromolecular structure.

481

482 Figure 6 Probable structure of molecules calculated from MALDI-ToF data.

483

484 3.5. Rheological behavior

485 The rheological measurements allowed characterizing the mathematical model
486 and rheological behavior of the synthesized bio-based poly(propylene succinate)s. The
487 tests were prepared at 60, 70 and 80°C and the shear rate at the range from 0 to 100
488 s^{-1} . The justification for the temperature and shear rate choice is due to the usually
489 used conditions during industrial processes. Figures 7 and 8 show the viscosity and
490 flow curves of the prepared polyester polyols, respectively. Moreover, Tables 4 and 5
491 present the mathematical models of the prepared polyols rheological behavior. For
492 more comprehensive results interpretation, rheological behavior of the POLIOS 55/20
493 was also investigated and presented in the figures and tables.

494

495 Figure 7 The viscosity curves of the synthesized bio-based polyester polyols and
496 POLIOS 55/20 at a) 60°C, b) 70°C, c) 80°C.

497

498 The viscosity curves showed the relationship between polyols viscosity and
499 shear rate. The results confirmed the non-Newtonian character of the measured
500 materials. In Figure 7, the initial viscosity trend behavior with increasing shear rate
501 indicates the pseudoplastic behavior of the measured polyols. The macromolecular
502 chain orientation caused by flow field can explain the observed shear thinning
503 behavior. In the flow field, the molecules are changing their direction by rotation. After
504 achieving the parallel position to the flow direction, the viscosity stays constant. The
505 obtained viscosity curves confirmed the decrease of the synthesized polyols viscosity
506 with the increasing temperature. Only POLIOS 55/20 viscosity stays approximately
507 with the same values at different temperatures. Interesting is the fact that the initial
508 viscosity trend behavior with increasing shear rate for POLIOS 55/20 increase with the
509 growing temperature. The highest viscosity, at all three temperatures, revealed polyols
510 PPS-0.15 and PPS-0.20, when the lowest POLIOS 55/20 and PPS-0.30. The sample
511 PPS-0.25 revealed similar viscosity value to PPS-0.10 at 60 and 70°C and clearly
512 lower, similar to PPS-0.30, at 80°C.

513
514 Figure 8 The flow curves of the synthesized bio-based polyester polyols and POLIOS
515 55/20 at a) 60°C, b) 70°C, c) 80°C. The black line means the rising curves and the gray
516 line means falling curves.

517
518 Fluids exhibited the non-linear flow curves are described as non-Newtonian
519 liquids. The changes in the viscosity value can be observed as the variation of the
520 tangent of the curve slope angle [34] at the flow curves. It is expressed by the equation
521 (4):

522 $\tan \alpha = \eta_0$ (4)

523 All measured polyols revealed the decreasing angle α with increasing
524 temperatures. The obtained results verified the decreasing viscosity of the prepared
525 bio-based polyester polyols with the growing temperature. It also confirmed that the
526 shear stress decreases with the increasing temperature. The highest value of the shear
527 stress disclosed the polyol samples PPS-0.15 at 60°C and PPS-0.20 at 70°C which
528 equaled ca. 1500 Pa for both polyols (Figure 8). Specimen PPS-0.20 exhibited
529 molecular structure which disenabled the rheological measurement with 100 s⁻¹ of the
530 shear rate at 60°C. The obtained results are related to the viscosity of the sample.
531 What is seen in Table 1, polyol PPS-0.20 exhibited one of the higher viscosity, above
532 14.5 Pas (at 70°C), from the measured polyols. The viscosity incidents to the
533 dispersion of the molecular weight (polydispersity) of the sample. The highest value of
534 the polydispersity (above 2.5 for PPS-0.20, Table 2) confirmed that the PPS-0.20
535 featured a lot of the macromolecules with the differential molecular weights.
536 Furthermore, the peak location for PPS-0.20 in Figure 4 suggests that the prepared
537 polyol shows the higher content of the macromolecules with larger molecular weight
538 than designed. Its caused that the polyol is more sticky at the same temperature
539 compared to other measured polyols (except the PPS-0.00).

540 The lowest shear stress occurred for all synthesized polyols at 80°C and
541 equaled 885 Pa for PPS-0.20, 615 Pa for PPS-0.15, 435 Pa for PPS-0.10, 341 Pa for
542 PPS-0.25, 282 Pa for PPS-0.30, and 233 Pa for POLIOS 55/20, respectively.
543 Nevertheless, for this temperature, the flow curves for all polyol samples disclosed the
544 most visible no overlapping curves courses. This phenomenon is related to the
545 thixotropic behavior which occurs with irreversible decreasing shear stress with time
546 for the constant shear rate. At this time the hysteresis loops are observed. The

547 thixotropic fluids are the non-Newtonian liquids which characterized the decreasing
548 viscosity with the constant shear rate. It is caused by a progressive decomposition of
549 the fluid's structure. Due to the irreversible character of the thixotropic fluids, the state
550 of balance can be achieved after the structure reconstruction. The small hysteresis is
551 visible for all samples in the initial part of the curves courses. For the higher value of
552 the shear rate, the flow curves exhibited the linear behavior. This observation caused
553 difficulties with the unequivocal ascertainment of the pseudoplastic behavior of the
554 measured polyols (Figure 8). Nevertheless, the rheological measurements allowed
555 characterizing the mathematical models of the synthesized bio-based polyester
556 polyols, which clearly determined the pseudoplasticity of the polyols (Table 4 and 5).

557 Except for the temperature influence on the thixotropic behavior, the addition of
558 the catalyst have also an impact on this phenomenon. It is visible that the biggest
559 hysteresis loops exhibited samples with 0.15 and 0.20 wt.% of the catalyst employment
560 during synthesis. For sample PPS-0.25 and PPS-0.30, the hysteresis loops are smaller
561 which result in the decreasing of the thixotropic behavior. The observed hysteresis is
562 due to the polydispersity of the obtained bio-based polyols. The high level of the
563 molecular weight macromolecules distribution hindered the macromolecules reversion
564 to the state before the test. Nevertheless, observed hysteresis loops are small enough
565 to the nonsignificant impact on the industrial processes.

566

567

568

569 Table 4 The Herschel, Bulkley functions based on the rheological data from prepared bio-based polyols and POLIOS 55/20.

POLYESTER POLYOL	TEMPERATURE [°C]	FUNCTION	YIELD STRESS, τ_0 [Pa]	CONSISTENCY INDEX, μ_{om} [Pas ⁿ]	THE FLOW INDEX, n [-]	STABILITY INDEX, R ² [-]	BEHAVIOR
PPS-0.00	90	$y = 0+99.3391*x^{1.0008}$	0	99.3391	1.0008	0.9999	Newtonian
PPS-0.10	60	$y = 0+9.6411*x^{1.0079}$	0	9.6411	1.0079	0.9999	Dilatant
	70	$y = 0+5.4014*x^{1.0060}$	0	5.4014	1.0060	0.9999	Dilatant
	80	$y = 0+4.1753*x^{1.0093}$	0	4.1753	1.0093	0.9999	Dilatant
PPS-0.15	60	$y = 54.5411+15.8369*x^{0.9858}$	54.5411	15.8369	0.9858	0.9996	Bingham plastic
	70	$y = 78.2383+9.0299*x^{0.9822}$	78.2383	9.0299	0.9822	0.9978	Bingham plastic
	80	$y = 115.1738+4.4440*x^{1.0244}$	115.1738	4.4440	1.0244	0.9925	Bingham plastic
PPS-0.20	60	-	-	-	-	-	-
	70	$y = 16.6613+14.8832*x^{0.9958}$	16.6613	14.8835	0.9958	0.9999	Bingham plastic
	80	$y = 16.1543+9.1918*x^{0.9874}$	16.1543	9.1918	0.9874	0.9874	Bingham plastic
PPS-0.25	60	$y = 8.5405+9.5392*x^{0.9960}$	8.5405	9.5392	0.9960	0.9999	Bingham plastic
	70	$y = 14.2074+5.1267*x^{1.0067}$	14.2074	5.1267	1.0067	0.9995	Bingham plastic
	80	$y = 24.1504+2.8562*x^{1.0226}$	24.1504	2.8562	1.0226	0.9966	Bingham plastic
PPS-0.30	60	$y = 13.8697+6.2816*x^{1.0062}$	13.8697	6.2816	1.0062	0.9997	Bingham plastic
	70	$y = 27.4123+3.2987*x^{1.0204}$	27.4123	3.2987	1.0204	0.9977	Bingham plastic
	80	$y = 76.472+1.2952*x^{1.1036}$	76.4720	1.2952	1.1036	0.9892	Bingham plastic
POLIOS 55/20	60	$y = 83.6282+0.6145*x^{1.1687}$	83.6282	0.6145	1.1687	0.9025	Bingham plastic
	70	$y = 129.0917+0.0752*x^{1.4844}$	129.0917	0.0752	1.4844	0.5949	Bingham plastic
	80	$y = 165.6580+0.0188*x^{1.6719}$	165.6580	0.0188	1.6719	0.3510	Bingham plastic

y – shear stress [Pa], x – shear rate [s⁻¹]

570

571



572 Table 5 The Ostwald-de Waele functions based on the rheological data from prepared bio-based polyols and POLIOS 55/20.

POLYESTER POLYOL	TEMPERATURE [°C]	FUNCTION	CONSISTENCY INDEX, K [Pas ⁿ]	THE FLOW INDEX, n [-]	STABILITY INDEX R ² [-]	BEHAVIOR
PPS-0.00	90	$y = 98.5614 * x^{1.0044}$	98.5614	1.0044	0.9999	Newtonian
PPS-0.10	60	$y = 9.5418 * x^{1.0094}$	9.5418	1.0094	0.9999	Dilatant
	70	$y = 5.1120 * x^{1.0191}$	5.1120	1.0191	0.9999	Dilatant
	80	$y = 3.9225 * x^{1.0242}$	3.9225	1.0242	0.9999	Dilatant
PPS-0.15	60	$y = 124.3603 * x^{0.4950}$	124.3603	0.495	0.9660	Pseudoplastic
	70	$y = 105.1657 * x^{0.4262}$	105.1657	0.4262	0.9696	Pseudoplastic
	80	$y = 127.6615 * x^{0.2980}$	127.6615	0.2980	0.9677	Pseudoplastic
PPS-0.20	60	-	-	-	-	-
	70	$y = 67.9241 * x^{0.6034}$	67.9241	0.6034	0.9605	Pseudoplastic
	80	$y = 41.7221 * x^{0.6025}$	41.7221	0.6025	0.9659	Pseudoplastic
PPS-0.25	60	$y = 40.9889 * x^{0.6437}$	40.9889	0.6437	0.9776	Pseudoplastic
	70	$y = 36.0143 * x^{0.5436}$	36.0143	0.5436	0.9679	Pseudoplastic
	80	$y = 9.0573 * x^{0.7791}$	9.0573	0.7791	0.9981	Pseudoplastic
PPS-0.30	60	$y = 47.641 * x^{0.4867}$	47.6410	0.4867	0.9376	Pseudoplastic
	70	$y = 11.1922 * x^{0.7527}$	11.1922	0.7527	0.9965	Pseudoplastic
	80	$y = 34.5608 * x^{0.4277}$	34.5608	0.4277	0.9910	Pseudoplastic
POLIOS 55/20	60	$y = 83.7755 * x^{0.1451}$	83.7755	0.1451	0.9639	Pseudoplastic
	70	$y = 82.6236 * x^{0.1806}$	82.6236	0.1806	0.9779	Pseudoplastic
	80	$y = 154.6387 * x^{0.0478}$	154.6387	0.0478	0.9878	Pseudoplastic

573 y – shear stress [Pa], x – shear rate [s^{-1}]

574 The mathematical models for all measured bio-based polyester polyols, at all
575 three temperatures, as an optimal function with the highest stability index, were defined
576 and collected in Table 4 and 5. The rheological models were determined for measured
577 polyols as Herschel, Bulkley, and Ostwald-de Waele. The first model from above-
578 mentioned described fluids with the yield stress, the second model – without yield
579 stress. Although more appropriate for polyurethane industry are fluids without yields
580 stress, the obtained results confirmed possibility to the synthesized polyester polyols
581 industry employment.

582 Table 4 presents the functions of the Herschel, Bulkley model. The bio-based
583 polyester polyol PPS-0.00 was measured at 90°C due to the high viscosity which
584 hindered the measurements at a lower temperature. This reference polyol exhibited
585 the Newtonian model of liquids. PPS-0.10 revealed the dilatant behavior at all three
586 temperatures. These behavior types were determined due to the zero yield stress and
587 the flow index, which was higher than 1. The Herschel, Bulkley model described the
588 pseudoplastic behavior of the fluid revealed the yield stress above 1. The yield stress
589 of bio-based polyester polyols with higher catalyst content than 0.10 wt.% increases
590 with the growing temperature. Only PPS-0.20 revealed approximately constant value
591 ca. 16 Pa. The lowest value of the yield stress from all measured polyols at 60 and
592 70°C exhibited PPS-0.25, which totaled ca. 8.5 and 14.2 Pa, respectively. At 80°C this
593 value for PPS-0.25 amounted to ca. 24 Pa. The consistency index is a measure of the
594 viscosity. The value of consistency index decreased with the temperature growing
595 except for this value for PPS-0.15, PPS-0.30 and POLIOS 55/20 at 80°C (Table 4).

596 The Ostwald-de Waele models, which are presented in Table 5 also confirmed
597 the Newtonian fluid behavior for PPS-0.00 and dilatant behavior for PPS-0.10. The
598 other measured polyols revealed pseudoplastic behavior due to the flow index value,



599 which was lower than 1 at all temperatures. Furthermore, the differences in the
600 behavior appellation for polyols from PPS-0.15 to PPS-0.30 in Table 4 and Table 5 are
601 related to the appropriate model character. The Bingham plastic behavior (Table 4)
602 describes fluids with the yield stress (Hershel, Bulkley model). The pseudoplastic
603 behavior depicts fluids without yield stress (Ostwald-de Waele model, Table 5).

604 The obtained results of the rheological measurements confirmed the most
605 desirable rheological behavior from the synthesized bio-based polyester polyols as a
606 polyol with the use of 0.25 wt.% of the catalyst.

607 4. Conclusion

608 The fully bio-based polyester polyols for polyurethane materials were
609 successfully synthesized via two-step polycondensation method. The optimization of
610 polycondensation process was based on the verification of the catalyst amount, which
611 led to the molecular structure characteristics and selective properties the most akin to
612 designed. The structure analysis via FTIR method confirmed that the content of the
613 catalyst nonsignificantly influenced on the macromolecular structure of the synthesized
614 polyols. The ^1H NMR measurements allowed verifying obtainment of the designed low
615 molecular weight polyesters as an occurrence of the little peaks named 'a', 'b', 'c' on
616 the ^1H NMR spectra of the synthesized poly(propylene succinate)s. The GPC analysis
617 confirmed that the fully bio-based polyols synthesized with the 0.25 wt.% and 0.30
618 wt.% catalyst content revealed the most desirable molecular weight distribution with
619 the ca. 1.8 polydispersity level and ca. 2500 g/mol number average molecular weight.
620 Mass spectrometry analysis proved to be a highly effective tool to facilitate the
621 identification of the molecular structure distribution of the prepared bio-based polyester
622 polyols as well as serve as a core method to investigate the impact of the catalyst
623 amount on the polyols structure development during synthesis. Through the

624 hyphenation of these sophisticated polymer characterization techniques, information
625 on the molecular heterogeneity of the obtained bio-based polyester polyols, showing a
626 complex variety of possible distributions, was obtained. Matrix-Assisted Laser
627 Desorption/Ionization Time-of-Flight mass spectrometry allowed confirming the impact
628 of the catalyst amount during synthesis on the molecular structure of the resulted
629 polyols. Moreover, it was found that the obtained polyols are non-Newtonian fluids,
630 which can be described as an optimal function by Herschel, Bulkley and Ostwald-de
631 Waele models. The obtained results of the rheological measurements confirmed the
632 desirable rheological behavior for the bio-based polyester polyol synthesized with the
633 use of 0.25 wt.% and 0.30 wt.% of the catalyst. These polyols revealed pseudoplasticity
634 with the lowest value of the yield stress at 60, 70 and 80°C. The conducted
635 investigations confirmed similarity of the prepared bio-based polyester polyols to the
636 commercially used synthetic polyester polyols proposed for flexible and thermoplastic
637 polyurethane materials.

638 Acknowledgments

639 Authors acknowledged the DuPont Tate&Lyle BioProducts (Loudon,
640 Tennessee, USA) for supplying the glycol (1.3-propanediol) samples used in this study.
641 Moreover, Authors gratefully acknowledge also receiving the samples of succinic acid
642 employed in this study from BioAmber Sarnia Inc. (Sarnia, Ontario, Canada).

643 Thanks are also due to Mrs. Professor Arantxa Eceiza and her research team
644 from the Department of Chemical and Environmental Engineering at the University of
645 the Basque Country for the Gel Permeation Chromatography measurements of the
646 bio-based polyester polyols described in this work.

647 The sincere acknowledgments are directed to the PURINOVA Sp. Z o.o.
648 (Bydgoszcz, Poland) for the Matrix-Assisted Laser Desorption/Ionization Time-of-
649 Flight mass spectrometry measurements of the bio-based polyester polyols described
650 in this work. Tests were conducted during the scientific and technological internship.

651 Funding

652 This research did not receive any specific grant from funding agencies in the
653 public, commercial, or not-for-profit sectors.

654 REFERENCES

- 655 [1] J.C. de Haro, J.F. Rodriguez, A. Perez, M. Carmona, Incorporation of azide
656 groups into bio-polyols, *J. Clean. Prod.* 138 (2016) 77–82.
657 doi:10.1016/j.jclepro.2016.05.012.
- 658 [2] R. Miller, Evaluating the Properties and Performance of Susterra® 1, 3
659 Propanediol and Biosuccinium™ Sustainable Succinic Acid in TPU
660 Applications, in: *CPI Polyurethanes 2012 Tech. Conf.*, 2012: pp. 1–19.
661 [http://www.reverdia.com/wp-content/uploads/Article-PUMI-](http://www.reverdia.com/wp-content/uploads/Article-PUMI-Biosuccinium_and_Susterra_03-2013.pdf)
662 [Biosuccinium_and_Susterra_03-2013.pdf](http://www.reverdia.com/wp-content/uploads/Article-PUMI-Biosuccinium_and_Susterra_03-2013.pdf).
- 663 [3] C. Delhomme, D. Weuster-Botz, F.E. Kühn, Succinic acid from renewable
664 resources as a C4 building-block chemical—a review of the catalytic
665 possibilities in aqueous media, *Green Chem.* 11 (2009) 13.
666 doi:10.1039/b810684c.
- 667 [4] I. Bechthold, K. Bretz, S. Kabasci, R. Kopitzky, A. Springer, Succinic acid: A
668 new platform chemical for biobased polymers from renewable resources,
669 *Chem. Eng. Technol.* 31 (2008) 647–654. doi:10.1002/ceat.200800063.

- 670 [5] S. V. Kamzolova, A.I. Yusupova, E.G. Dedyukhina, T.I. Chistyakova, T.M.
671 Kozyreva, I.G. Morgunov, Succinic acid synthesis by ethanol-grown yeasts,
672 Food Technol. Biotechnol. 47 (2009) 144–152.
- 673 [6] N. Nghiem, B. Davison, B. Suttle, G. Richardson, Production of succinic acid
674 by Anaerobiospirillum succiniciproducens, Apply Biochem. Biotechnol. 63/65
675 (1997) 565–576. <http://www.ncbi.nlm.nih.gov/pubmed/24409768>.
- 676 [7] L. Montero de Espinosa, M. Meier, J. Ronda, M. Galia, V. Cadiz, Phosphorus-
677 Containing Renewable Polyester-Polyols via ADMET Polymerization:
678 Synthesis, Functionalization, and Radical Crosslinking, J. Polym. Sci. Part A
679 Polym. Chem. 48 (2010) 1649–1660. doi:10.1002/pola.
- 680 [8] J. Djonlagic, M.S. Nolic, Chapter 6: Biodegradable polyesters: Synthesis and
681 Physical Properties, in: A Handb. Appl. Biopolym. Technol. Synth. Degrad.
682 Appl., Royal Society of Chemistry, United Kingdom, 2011: pp. 149–196.
- 683 [9] D.N. Bikiaris, D.S. Achilias, Synthesis of poly(alkylene succinate)
684 biodegradable polyesters, Part I: Mathematical modelling of the esterification
685 reaction, Polymer (Guildf). 47 (2006) 4851–4860.
686 doi:10.1016/j.polymer.2008.06.026.
- 687 [10] M. Ionescu, Chemistry and Technology of Polyols for Polyurethane, First Edit,
688 Rapra Technology Limited, United Kingdom, 2005. doi:10.1002/pi.2159.
- 689 [11] N.E. Alexander, J.P. Swanson, A. Joy, C. Wesdemiotis, Sequence analysis of
690 cyclic polyester copolymers using ion mobility tandem mass spectrometry, Int.
691 J. Mass Spectrom. (2017). doi:10.1016/j.ijms.2017.07.019.

- 692 [12] A.P. Gies, S.M. Stow, J.A. McLean, D.M. Hercules, MALDI-TOF/TOF CID
693 study of poly(1,4-dihydroxybenzene terephthalate) fragmentation reactions,
694 Polymer (Guildf). 64 (2015) 100–111. doi:10.1016/j.polymer.2015.03.021.
- 695 [13] R. Medimagh, S. Mghirbi, A. Saadaoui, A. Fildier, M. Desloir-Bonjour, G. Raffin,
696 H.R. Kricheldorf, S. Chatti, Synthesis of biosourced polyether-amides from 1,4-
697 3,6-dianhydrohexitols: Characterization by NMR and MALDI-ToF mass
698 spectrometry, Comptes Rendus Chim. 16 (2013) 1127–1139.
699 doi:10.1016/j.crci.2013.05.004.
- 700 [14] H. Ben Abderrazak, A. Fildier, S. Marque, D. Prim, H. Ben Romdhane, H.R.
701 Kricheldorf, S. Chatti, Cyclic and non cyclic aliphatic-aromatic polyesters
702 derived from biomass: Study of structures by MALDI-ToF and NMR, Eur.
703 Polym. J. 47 (2011) 2097–2110. doi:10.1016/j.eurpolymj.2011.07.009.
- 704 [15] L. Chikh, M. Tessier, A. Fradet, NMR and MALDI-TOF MS study of side
705 reactions in hyperbranched polyesters based on 2,2-
706 bis(hydroxymethyl)propanoic acid, Polymer (Guildf). 48 (2007) 1884–1892.
707 doi:10.1016/j.polymer.2007.02.019.
- 708 [16] P. Król, B. Pilch-Pitera, Urethane oligomers as raw materials and intermediates
709 for polyurethane elastomers. Methods for synthesis, structural studies and
710 analysis of chemical composition, Polymer (Guildf). 44 (2003) 5075–5101.
711 doi:10.1016/S0032-3861(03)00431-2.
- 712 [17] P. Król, B. Pilch-Pitera, Study on the synthesis of urethane oligomers as
713 intermediate products for the production of linear polyurethanes, Eur. Polym. J.
714 37 (2001) 251–266. doi:10.1016/S0014-3057(00)00116-6.

- 715 [18] E. Głowińska, J. Datta, A mathematical model of rheological behavior of novel
716 bio-based isocyanate-terminated polyurethane prepolymers, *Ind. Crops Prod.*
717 60 (2014) 123–129. doi:10.1016/j.indcrop.2014.06.016.
- 718 [19] A. Björn, P. Segura, D. La Monja, A. Karlsson, J. Ejlertsson, B.H. Svensson,
719 Rheological Characterization, *Intech.* (2012) 64–76. doi:10.5772/32596.
- 720 [20] A.K. Schrock, H.S.C. Hamilton, B.D. Thompson, K. Ulrich, C. del Rosario, C.J.
721 Saint-Louis, W.D. Coggio, Development of structure–property relationships that
722 allow independent control of glass transition temperature, melting temperature,
723 and rheology in a library of bio-based succinate polyester polyols, *Polymer*
724 (Guildf). 114 (2017) 103–112.
725 doi:http://dx.doi.org/10.1016/j.polymer.2017.02.092.
- 726 [21] N. Triantafillopoulos, *Measurement of Fluid Rheology and Interpretation of*
727 *Rheograms*, Second Edi, Kaltec Scientific, Inc., Novi, Michigan, USA, 1988.
- 728 [22] PURINOVA, <http://www.purinova.com/>, (2017).
- 729 [23] L. Zheng, C. Li, D. Zhang, G. Guan, Y. Xiao, D. Wang, Multiblock copolymers
730 composed of poly (butylene succinate) and poly (1 , 2-propylene succinate):
731 Effect of molar ratio of diisocyanate to polyester-diols on crosslink densities ,
732 thermal properties , mechanical properties and biodegradability, *Polym.*
733 *Degrad. Stab.* 95 (2010) 1743–1750.
734 doi:10.1016/j.polymdegradstab.2010.05.016.
- 735 [24] S.S. Umare, A.S. Chandure, R.A. Pandey, Synthesis, characterization and
736 biodegradable studies of 1,3-propanediol based polyesters, *Polym. Degrad.*
737 *Stab.* 92 (2007) 464–479. doi:10.1016/j.polymdegradstab.2006.10.007.

- 738 [25] X. Ma, P.R. Chang, J. Yu, N. Wang, Preparation and properties of
739 biodegradable poly (propylene carbonate)/ thermoplastic dried starch
740 composites, Carbohydr. Polym. 71 (2008) 229–234.
741 doi:10.1016/j.carbpol.2007.05.033.
- 742 [26] D.N. Bikiaris, G.Z. Papageorgiou, D.S. Achilias, Synthesis and comparative
743 biodegradability studies of three poly(alkylene succinate)s, Polym. Degrad.
744 Stab. 91 (2006) 31–43. doi:10.1016/j.polymdegradstab.2005.04.030.
- 745 [27] D.N. Bikiaris, G.Z. Papageorgiou, D.J. Giliopoulos, C.A. Stergiou, Correlation
746 between Chemical and Solid-State Structures and Enzymatic Hydrolysis in
747 Novel Biodegradable Polyesters . The Case of Poly (propylene
748 alkanedicarboxylate) s, Macromol. Bioscience. 8 (2008) 728–740.
749 doi:10.1002/mabi.200800035.
- 750 [28] K. Chrissafis, K.M. Paraskevopoulos, D.N. Bikiaris, Thermal degradation
751 kinetics of the biodegradable aliphatic polyester, poly(propylene succinate),
752 Polym. Degrad. Stab. 91 (2006) 60–68.
753 doi:10.1016/j.polymdegradstab.2005.04.028.
- 754 [29] K. Chrissafis, K.M. Paraskevopoulos, D.N. Bikiaris, Thermal degradation
755 mechanism of poly(ethylene succinate) and poly(butylene succinate):
756 Comparative study, Thermochim. Acta. 435 (2005) 142–150.
757 doi:10.1016/j.tca.2005.05.011.
- 758 [30] L. Zheng, C. Li, W. Huang, X. Huang, Synthesis of high-impact biodegradable
759 multiblock copolymers comprising of poly (butylene succinate) and
760 hexamethylene diisocyanate as chain extender, Polym. Adv. Technol. 22

- 761 (2011) 279–285. doi:10.1002/pat.1530.
- 762 [31] P. Kopczyńska, J. Datta, Single-phase product obtained via crude glycerine
763 depolymerisation of polyurethane elastomer: Structure characterisation and
764 rheological behaviour, *Polym. Int.* 65 (2016) 946–954. doi:10.1002/pi.5128.
- 765 [32] N.O. Pretorius, K. Rode, J.M. Simpson, H. Pasch, Analysis of complex phthalic
766 acid based polyesters by the combination of size exclusion chromatography
767 and matrix-assisted laser desorption/ionization mass spectrometry, *Anal. Chim.*
768 *Acta.* 808 (2014) 94–103. doi:10.1016/j.aca.2013.07.030.
- 769 [33] J.C. Soutif, N.T.H. Doan, V. Montembault, Determination by MALDI-TOF MS of
770 the structures obtained from polytransesterification of diethyl 2,6-
771 pyridinedicarboxylate and poly(ethylene glycol), *Eur. Polym. J.* 42 (2006) 126–
772 132. doi:10.1016/j.eurpolymj.2005.07.026.
- 773 [34] K. Wilczyński, *Reologia w przetwórstwie tworzyw sztucznych*, Wydawnictwo
774 Naukowo-Techniczne, Warszawa, 2001.

775

776

777 Caption of Figures

778 Figure 1 Two-step polycondensation method for poly(propylene succinate)
779 obtainment.

780 Figure 2 FTIR spectra of the used succinic acid, 1,3-propanediol, and selected
781 poly(propylene succinate)s.

782 Figure 3 ^1H NMR spectrum of the synthesized poly(propylene succinate)s samples.

783 Figure 4 GPC spectra of the synthesized poly(propylene succinate)s.

784 Figure 5 MALDI-ToF spectra of the bio-based poly(propylene succinate)s: a) PPS-
785 0.00, b) PPS-0.10, c) PPS-0.15, d) PPS-0.20, e) PPS-0.25, f) PPS-0.30.

786 Figure 6 Probable structure of molecules calculated from MALDI-ToF data.

787 Figure 7 The viscosity curves of the synthesized bio-based polyester polyols and
788 POLIOS 55/20 at a) 60°C, b) 70°C, c) 80°C.

789 Figure 8 The flow curves of the synthesized bio-based polyester polyols and POLIOS
790 55/20 at a) 60°C, b) 70°C, c) 80°C. The black line means the rising curves and the gray
791 line means falling curves.

792

793 Caption of Tables

794 Table 1 Preparation and properties of the obtained bio-based polyester polyols and
795 POLIOS 55/20.

796 Table 2 The results of the GPC measurements.

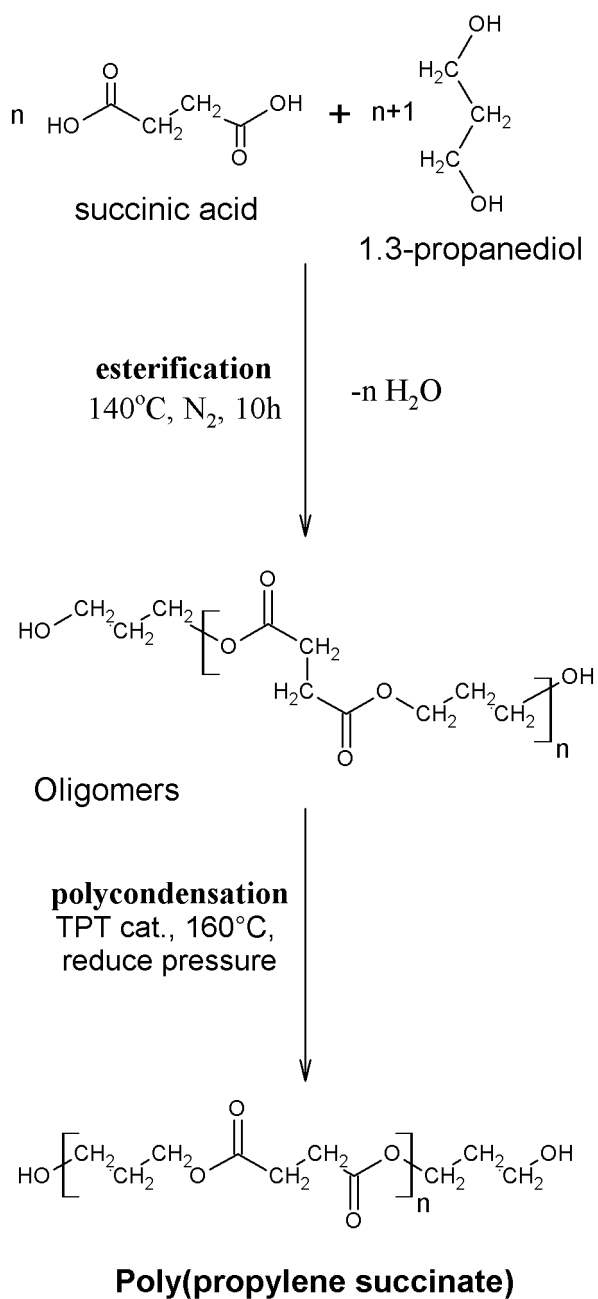
797 Table 3 Interpretation of MALDI-ToF mass spectra for obtained bio-based polyester
798 polyols.

799 Table 4 The Herschel, Bulkley functions based on the rheological data from prepared
800 bio-based polyols and POLIOS 55/20.

801 Table 5 The Ostwald-de Waele functions based on the rheological data from prepared
802 bio-based polyols and POLIOS 55/20.

803

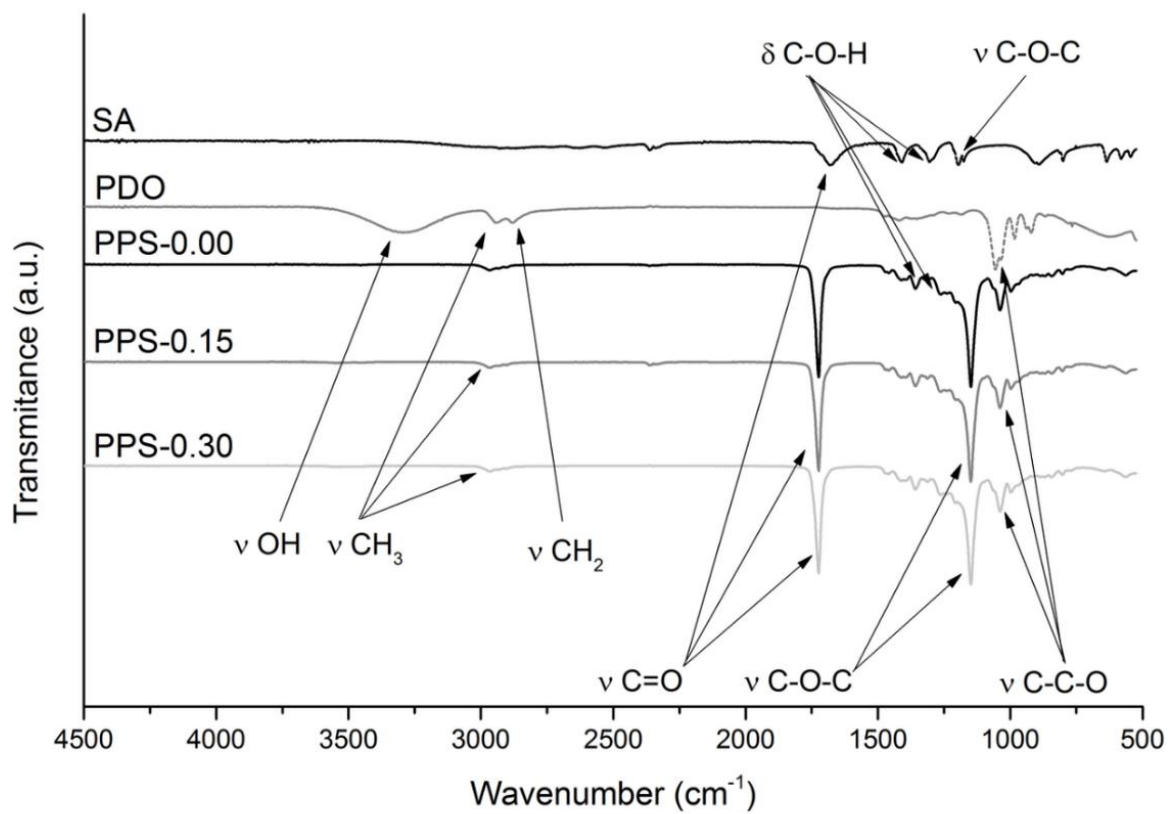
804 Figure 1



805

806

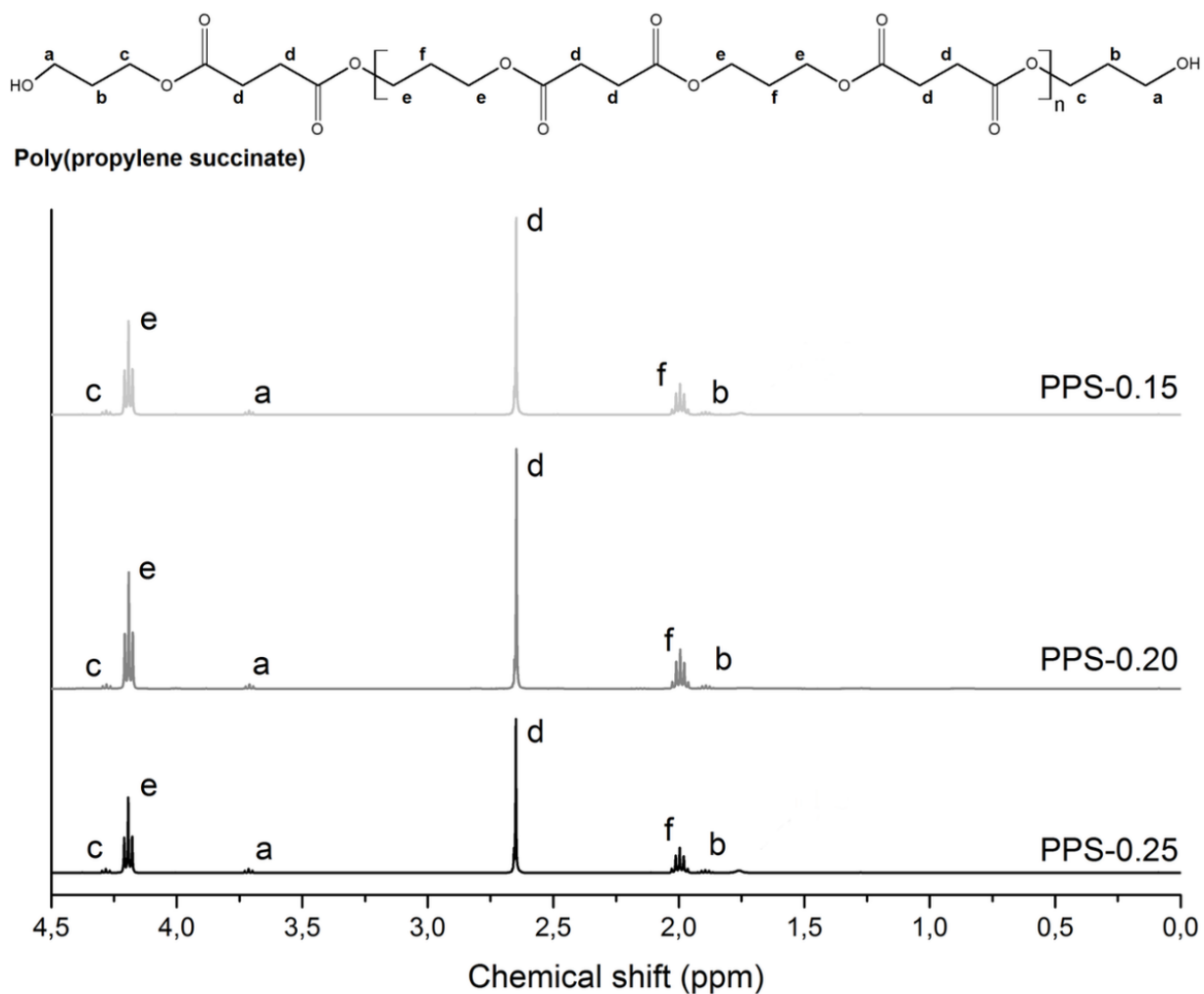
807 Figure 2



808

809

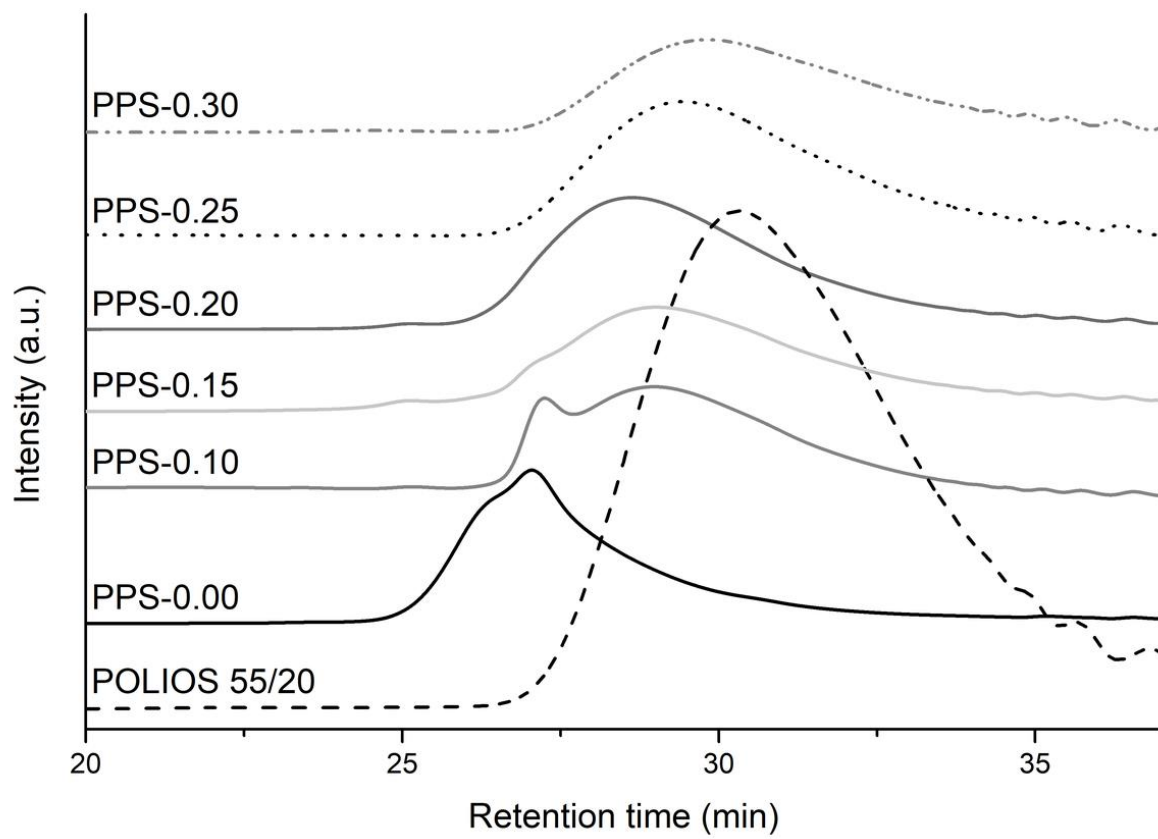
810 Figure 3



811

812

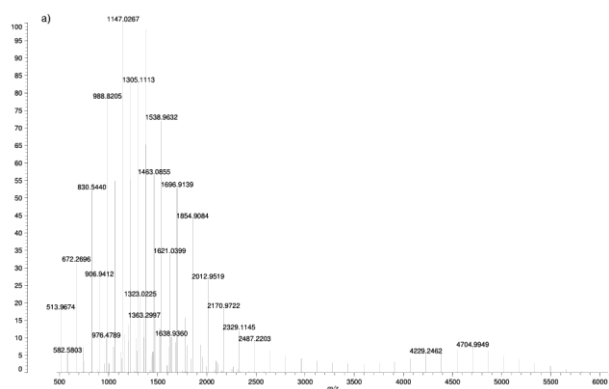
813 Figure 4



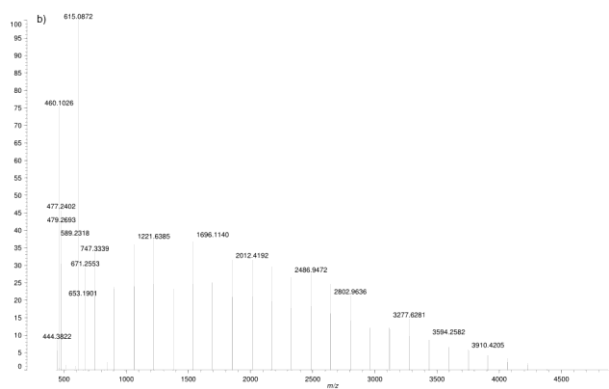
814

815

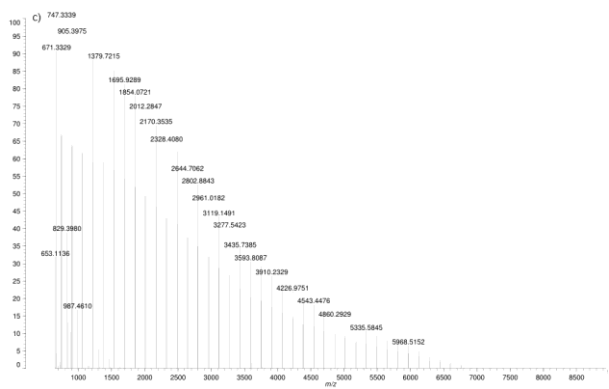
816 Figure 5



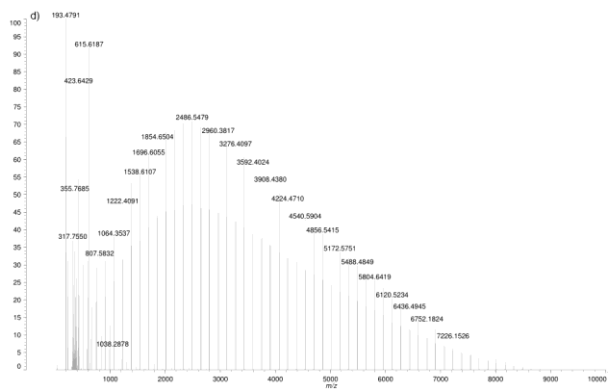
817



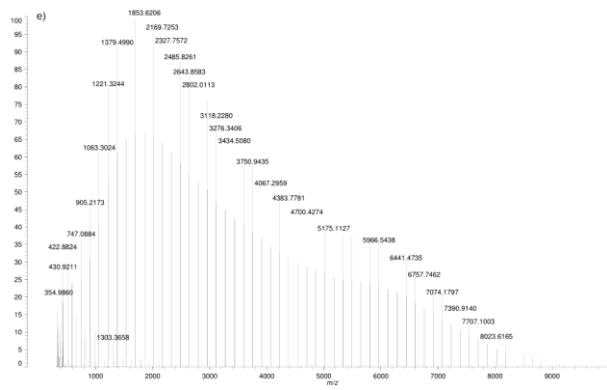
818



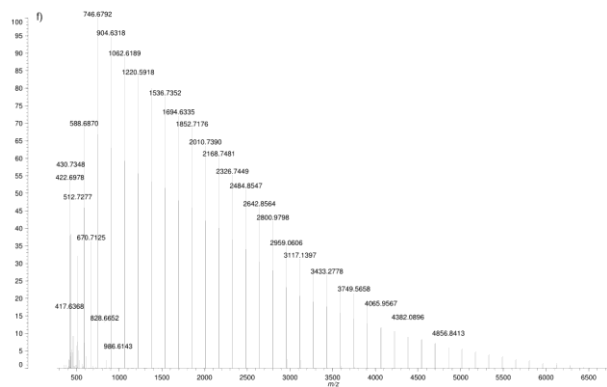
819



820



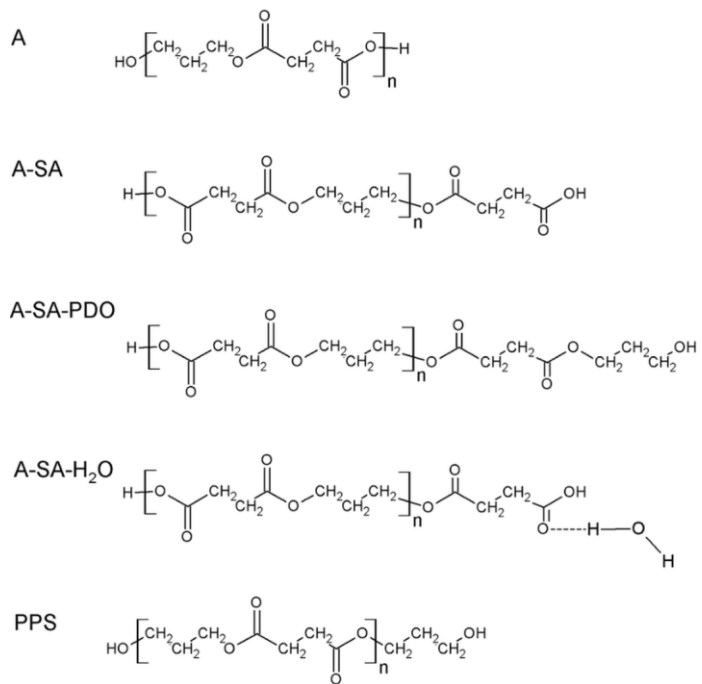
821



822

823

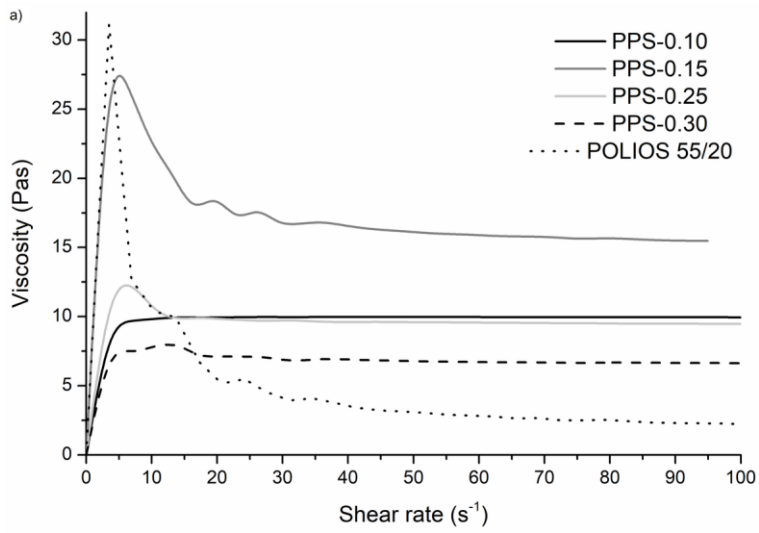
824 Figure 6



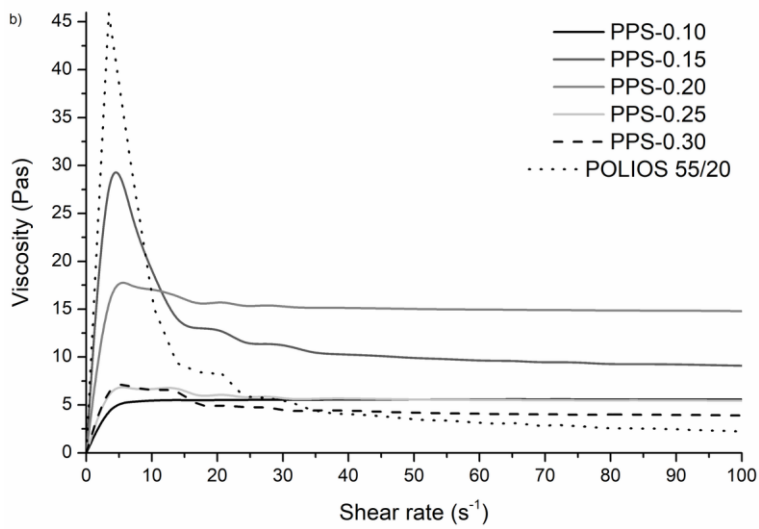
825

826

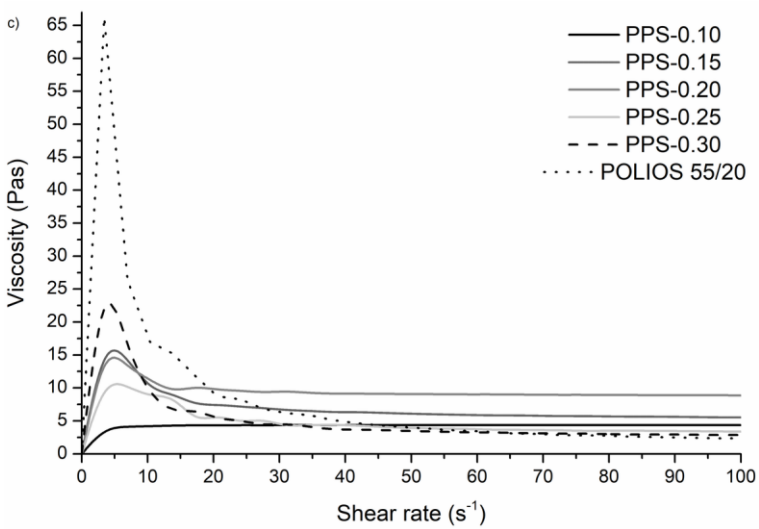
827 Figure 7



828



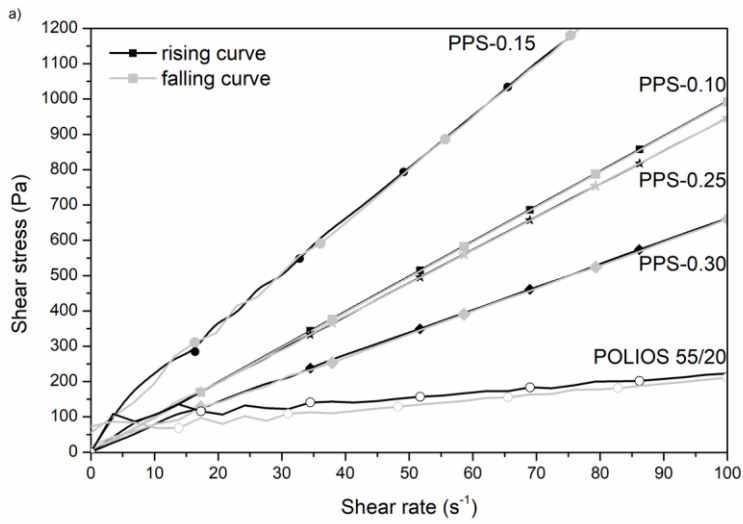
829



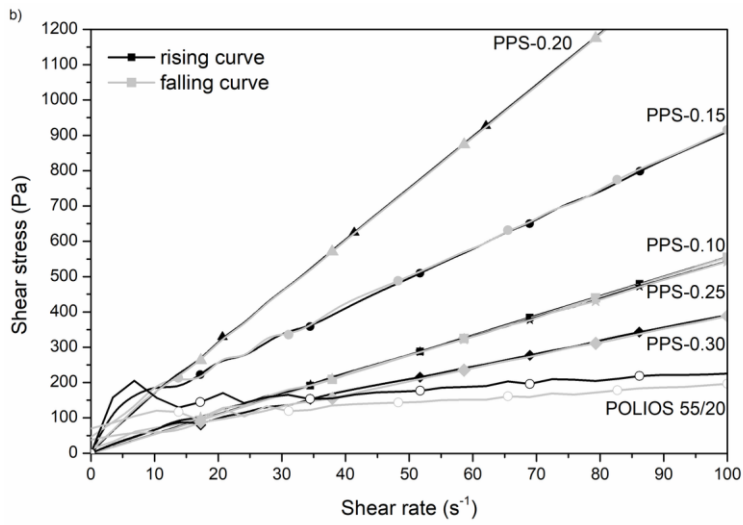
830

831

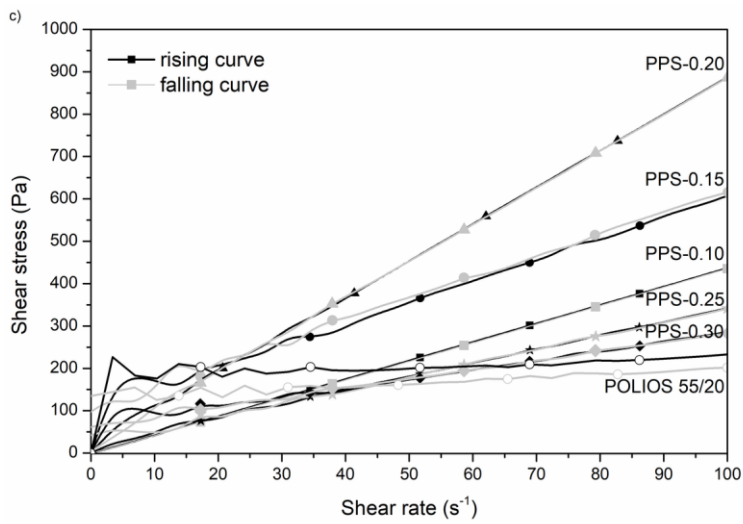
832 Figure 8



833



834



835

836

